

Rapidly solidified Ag-Cu eutectics: A comparative study using drop-tube and melt fluxing techniques

Y Yu^a, A M Mullis^b and R F Cochrane^c

Institute for Materials Research, University of Leeds, Leeds, LS2 9JT, UK.

Email: ^apmysy@leeds.ac.uk, ^bA.M.Mullis@leeds.ac.uk, ^cr.f.cochrane@leeds.ac.uk

Abstract. A comparative study of rapid solidification of Ag-Cu eutectic alloy processed via melt fluxing and drop-tube techniques is presented. A computational model is used to estimate the cooling rate and undercooling of the free fall droplets as this cannot be determined directly. SEM micrographs show that both materials consist of lamellar and anomalous eutectic structures. However, below the critical undercooling the morphologies of each are different in respect of the distribution and volume of anomalous eutectic. The anomalous eutectic in flux-undercooled samples preferentially forms at cell boundaries around the lamellar eutectic in the cell body. In drop-tube processed samples it tends to distribute randomly inside the droplets and at much smaller volume fractions. That the formation of the anomalous eutectic can, at least in part, be suppressed in the drop-tube is strongly suggestive that the formation of anomalous eutectic occurs via remelting process, which is suppressed by rapid cooling during solidification.

1. Introduction

Ag-Cu eutectic alloys have been widely studied for their remarkable strength and conductivity under both near-equilibrium and rapid solidification conditions. As one of the simplest binary eutectic systems, with the same face-centred cubic crystal structure in both the Cu-rich and Ag-rich phases, it is ideally suited for the study of rapid solidification behaviour. Various containerless processing techniques, such as splat quenching, drop tube processing, electromagnetic levitation and melt fluxing have been used to achieve high undercooling in Ag-Cu droplets [1]. In melt fluxing, high undercoolings may be achieved after thermal cycling to remove possible impurities attached on the melt surface, but during post-recalcrescence solidification the highest cooling rate achieved is typically no more than 10 K s^{-1} [2], leading to significant post-recalcrescence modification of the original solidification structure [3]. Conversely, in drop-tube processing, a range of cooling rates from 10^3 to 10^6 K s^{-1} is achieved via the production of a fine spray of free falling droplets of varying sizes [4]. However, determination of the nucleation temperature, and hence the undercooling within individual droplets is not possible. Therefore, an indirect method of estimating these quantities from the size of the as-solidified droplet may be employed, details of which are given in [1, 5].

The mechanism of anomalous eutectic formation during rapid solidification has been the subject of controversy for many years. In Ag-Cu, most such studies have mainly concentrated on the condition of low undercooling. The highest undercooling in which the formation of anomalous eutectic is observed in Ag-Cu has been variously reported as 70 K [6], 75 K [3] and 76 K [7], with higher undercoolings resulting in the formation of supersaturated single-phase dendrites instead. Wang et al [8] also estimated a maximum undercooling of 70 K in drop-tube processed samples, in agreement with the results of direct undercooling studies. At intermediate undercoolings, less than the critical



undercooling [9] and typically < 60 K [10], it has been widely conjectured that the initial planar eutectic front breaks down into several eutectic dendritic tips ahead of S/L interface. The rapid release of latent heat associated with this rapid growth may then remelt the initially formed eutectic dendrite giving the observed anomalous eutectic.

In this paper, the microstructure of Ag-Cu alloy droplets that have been rapidly solidified by drop-tube processing will be compared with the results of our previous investigation [6] in which melt fluxing was used to undercool an alloy of the same eutectic composition. The cooling rate and undercoolings of droplets formed during drop-tube processing are calculated as a function of particle size which may in turn provide new insights into the mechanism of anomalous eutectic formation.

2. Experimental methods

Rapid solidification of Ag-Cu eutectic alloy was studied in a 6.5 m drop-tube. In order to achieve high undercoolings, a thin liquid jet fell uncontained through the tube in an atmosphere of dried, oxygen-free N_2 gas to solidify as small droplets at the bottom of the tube.

A high-purity ingot of Ag-28 wt. %Cu eutectic alloy was prepared from 99.99% purity silver and copper shot. The Ag-Cu eutectic sample was placed in a 10 mm diameter and 20 mm long alumina crucible with 3 laser drilled holes in the base, each of which was 300 μm in diameter. This was then fixed at the top of the drop-tube surrounded by the RF coils. Prior to backfilling with purified nitrogen gas at 400 kPa, the tube was evacuated to a pressure of < 1 Pa by an oil-sealed rotary-vane pump and then to 10^{-4} Pa using a turbo-molecular pump. Following evacuation and backfilling the ingot was melted by RF induction heating of a graphite susceptor. When the desired superheat was obtained the melt was forced through the holes in the crucible base using 0.4 MPa N_2 gas. The various sizes of droplets were collected at the bottom of the drop-tube once they had cooled to ambient temperature. Further details of the experimental procedure are given in [4].

The droplets were sieved into the following size ranges; 850, 700, 500, 300, 212, 150, 106 μm , following which they were hot mounted and ground on a series of progressively finer SiC papers and polished using diamond paste. The morphologies of well-polished sample were subsequently characterized by means of SEM backscattered-electron imaging and EDX mapping.

3. Computational calculation

Due to the absence of an effective method for the direct observation of the formation of droplets in flight, computational methods are used to predict the process of droplet solidification and to provide a better physical understanding of the effect of experimental parameters upon the solidification morphology. The equation for the cooling rate, \dot{T} , as a function of volume, v_s , of droplet is given in equation (1) [11], where ρ_l is the mass density of the melt, C_p^l the specific heat of the liquid, and h_m the heat transfer coefficient. For the prediction of undercooling ΔT , as a function of diameter D we use the heat transfer model proposed by Lee and Ahn [5] as given equation (2). In order to estimate the wetting angle factor, $f(\theta)$, as a function of the droplet size, we use the empirical expression given by equation (3) [12]. All thermal physical parameters of Ag-Cu alloy and nitrogen gas have been obtained from [4, 5] respectively.

$$\dot{T} = \frac{1}{v_s \rho_l C_p^l \delta T} \int_{T_o}^{T_n} [h_m (T - T_R) + \varepsilon \sigma_{SB} (T^4 - T_R^4)] \cdot dT \quad (1)$$

$$\frac{\Psi(\theta)}{T_N \cdot \Delta T^2} = \ln \Phi(T_N, \theta, D) \quad (2)$$

$$f(\theta) = -0.0307 + \frac{35.5212}{D} \quad (3)$$

The calculated cooling rate and undercooling against droplet diameter is plotted in figure 1. It can be seen that with increasing droplet size there is a decline in the level of both undercooling and cooling rate, as expected [1]. We note however that the cooling rates calculated here are significantly lower than those given in [4]. This is due to the different inert gas chosen as a protective environment. As the specific heats of nitrogen and helium are $1039 \text{ J kg}^{-1} \text{ K}^{-1}$ and $5195 \text{ J kg}^{-1} \text{ K}^{-1}$ respectively, the heat transfer from the sample to the environment is much more rapid in helium than in nitrogen.

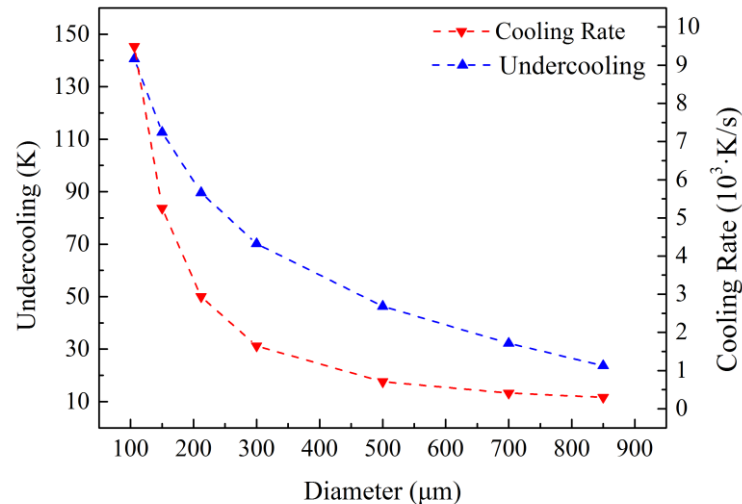


Figure 1. Calculated relationship between diameter, cooling rate (left Y-axis) and maximum undercooling (right Y-axis). Interpolation of the curves is only provided to guide the eye. The estimated cooling rate decreases from $9.50 \times 10^3 \text{ K s}^{-1}$ to $0.30 \times 10^3 \text{ K s}^{-1}$ over the range of droplet size produced in the drop-tube.

4. Results

In samples processed by melt fluxing there is extensive evidence for anomalous eutectic formation, as shown in figure 2(a), in which the microstructure is typically cellular, with cells consisting of lamellar eutectic in the cell body and anomalous eutectic occurring at the cell boundaries. In contrast, the anomalous eutectic formed in drop tube processed samples has a less clear distinction between these morphologies. With reference to figure 2(b), we note that the formation of colonies of lamellar eutectic, in the size range $10 \sim 20 \mu\text{m}$, are favoured inside droplets. More interestingly, there are numerous $2 \sim 5 \mu\text{m}$ Ag-rich regions formed at, or near, the colony boundaries, which appear as white spots in the micrograph due to Ag having a higher atomic number than Cu. These are not observed in the flux undercooled samples (figure 2(a)), despite each experiment using material from the same, fully homogenized, ingot of master alloy. In bulk undercooled alloys it is normally accepted that volume fraction of anomalous eutectic is a monotonically increasing function of the undercooling [3, 9]. In contrast, in drop-tube processed samples the volume fraction of anomalous eutectic shows no clear trend with particle size, which is a good proxy for both cooling rate and undercooling.

With decreasing droplet size it is much more likely that individual droplets will achieve higher undercooling during drop-tube processing due to the melt sub-division effect. This is clearly illustrated in figures 2(c), (d) and (e). It can be seen that the formation of single-phase dendrites becomes increasingly intense with decreasing droplet size, which is clearly indicative of increasing undercooling. In comparison with the morphology of figure 2(b), the microstructure displayed in figures 2(d) and (e) is clearly indicative of a different mechanism for microstructure formation above a critical undercooling of order of $70 \sim 90 \text{ K}$. Similar findings for melt-fluxed samples are presented in [3, 6, 7, 9], in which the supersaturated single-phase dendrite is formed as the primary phase in samples undercooled above the critical undercooling of $\sim 70 \text{ K}$.

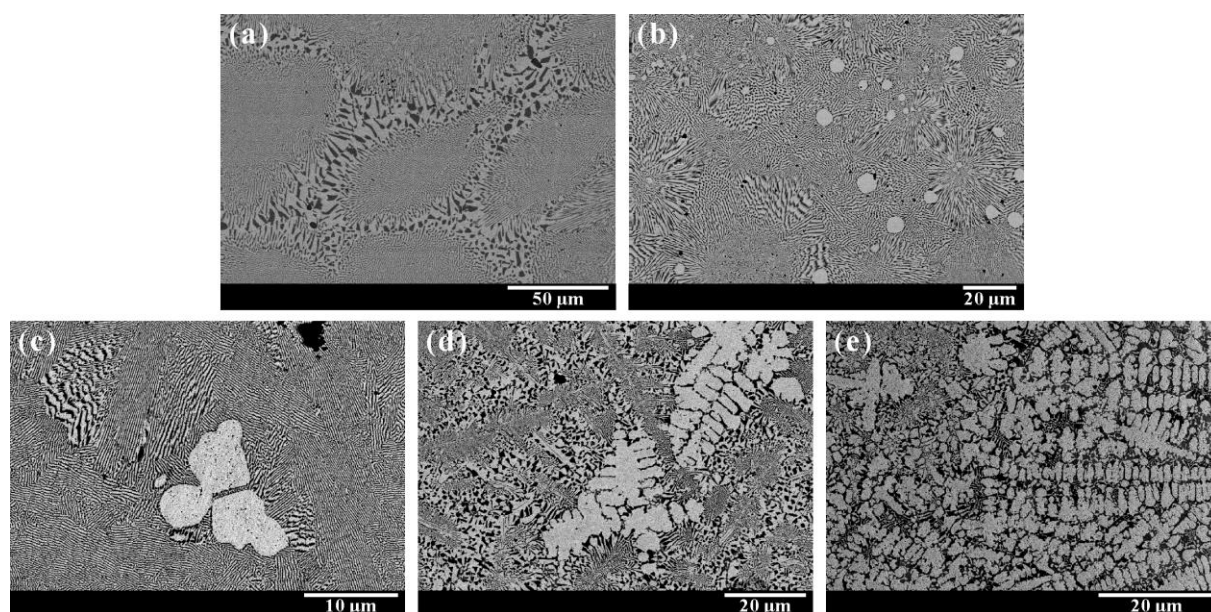


Figure 2. Series of micrographs showing the different morphologies via melt fluxing technique at (a) with undercooling 40K and drop-tube technique at (b) with the quantitative calculated undercooling in the droplet of the order of 30 K. With the decrease of droplet size, the Ag-rich single dendrite at figure (c) becomes increasingly dominant from figure (d) to figure (e).

5. Discussion

Above the critical undercooling samples produced by both melt fluxing and drop-tube processing clearly display single-phase dendrites as the primary solidification morphology, followed by the nucleation and growth of lamellar eutectic to fill the interdendritic space. Depending on the subsequent liquid temperature, anomalous eutectic formation might occur due to the remelting of either primary dendrites, or the subsequent interdendritic eutectic. In the case of drop-tube formed samples, the high cooling rate accompanying high undercooling appears favourable to the original solidification structure being retained, as shown in figure 2(d) and (e).

Conversely, the mechanism for anomalous eutectic formation for undercoolings less than 60 K via melt fluxing (or other bulk undercooling techniques) is most plausibly understood via the formation, and subsequent remelting, of eutectic cells or eutectic dendrites [6], with lamellar eutectic growing to infill the residual intercellular or interdendritic spaces. For similar undercoolings the microstructure obtained via drop-tube processing shows considerable difference to that obtained by melt fluxing, as can be seen by comparing figure 2(b) with figure 2(a). In particular, the eutectic grows in clearly defined colonies with numerous Ag-rich inclusions at or near the boundaries of the eutectic colonies. A reasonable explanation of the Ag-rich region formation should therefore play a central role in better understanding the mechanism of anomalous eutectic formation.

Figure 3(a) shows that the Ag-rich inclusions appear to be intimately related to the anomalous eutectic, merging seamlessly with the Ag-rich portion of the anomalous structure (figure 3(b) shows the EDX map for the same region, confirming that the inclusion is indeed Ag-rich). With reference to the metastable Ag-Cu phase diagram [14] we note that, for a eutectic formed from its undercooled parent melt, the Ag-rich phase will be supersaturated in Cu, but that the Cu-rich phase will still be close to, or slightly below, its equilibrium concentration of Ag. Upon reheating to the eutectic temperature, the Ag-rich phase will partially remelt while the Cu-rich phase will remain fully solid, but may of course be subject to coarsening. With the subsequent nucleation and growth of lamellar eutectic along the two-phase dendrite interface, the residual liquid will be Ag-rich, relative to the

eutectic composition, plausibly giving rise to the observed Ag-rich inclusions at the colony boundaries.

The measurement of lamellar spacing permits an estimation of the conditions under which lamellar eutectic growth occurred in the post-recalescence period. Our past work [10] relying on the Jackson-Hunt model strongly suggests that for flux undercooled samples the post-recalescence lamellar growth is independent of both the bulk undercooling of the sample and position within the sample. It was found that growth occurred within a very narrow range of lamellar spacing and with an indicative undercooling of around 4 K. This can be seen in the central cellular structure in figure 2(a), where the lamellar eutectic has an almost constant spacing of $\sim 0.28 \mu\text{m}$. In contrast, figure 2(b) shows that the lamellar eutectic spacing in drop-tube processed samples is dependent upon their location within the colony. A comparison of lamellar eutectic spacing in the different colonies by means of image analysis indicates that the lamellar spacing varies from around $0.56 \mu\text{m}$ to the nano-scale. This difference in lamellar spacing between the melt fluxing and the drop-tube techniques is suggestive that in the free falling droplets less time is available for the lamellar growth phase, which is consistent with the expected high cooling rate. We note with reference to figure 3(a) that the coarsest lamellar eutectic is either near the anomalous eutectic or attached to the Ag-rich spot, with a gradual decrease in lamellar spacing with distance away from each of those two areas.

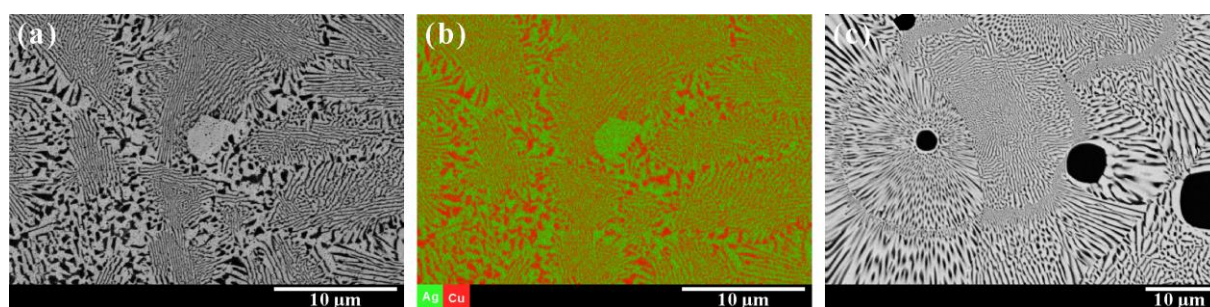


Figure 3. Micrographs showing different morphologies between droplets with fully molten liquid prior to free fall (a) and those with partially molten liquid prior to free fall (c). In order to clearly determine the composition distribution in the selected area (a), EDX mapping (b) is used as extensive evidence of droplet morphology, where green indicates Ag-rich regions and red Cu-rich regions.

Finally, we consider the possibility that the inclusions did not form from the melt, but instead were already present in the melt in the form of small unmelted fragments. To test this we performed a drop-tube run in which the master alloy was not fully melted prior to ejection. Figure 3(c) displays an example microstructure in which there was residual solid in the melt upon ejection during the drop-tube experiment. Firstly, we note that Cu-rich, rather than Ag-rich, inclusions are observed, a result of this being the high melting point phase. Secondly, it can be seen from figure 3(c) that the eutectic colonies radiate out from the solid Cu-rich inclusions which act as nuclei for solidification. This is contrary to the Ag-rich inclusion case, where the inclusions tend to cluster at colony boundaries, indicating they were one of the last features to solidify. Additionally, in this experiment no high undercooling (single phase dendrite) morphologies were observed, due to the strong heterogeneous nucleation effect within the droplets.

6. Conclusion

A comparative study on the solidification of Ag-Cu eutectic alloy via drop-tube and melt fluxing techniques has been undertaken and the results have been shown to yield useful insights into the formation of the anomalous eutectic morphology. Further work is in progress to determine the composition of Ag-rich region and to determine whether this correlates with the estimated undercooling within the droplets.

References

- [1] Herlach D M, Cochrane, R F, Egry I, Fecht H J, Greer A L 1993 *International Materials Reviews* **38** 273-347.
- [2] Çadirli E, Herlach D M, Volkmann T 2010 *Journal of Non-Crystalline Solids* **356** 461-466.
- [3] Walder S, Ryder P L 1993 *Journal of Applied Physics* **73** 1965-1970.
- [4] Erol M, Büyük U, Volkmann T, Herlach D M 2013 *Journal of Alloys and Compounds* **575** 96-103.
- [5] Lee E S, Ahn S 1994 *Acta Metallurgica Et Materialia* **42** 3231-3243.
- [6] Clopet C R, Cochrane R F, Mullis A M 2013 *Applied Physics Letters* **102** 031906.
- [7] Walder S, Ryder P L 1993 *Journal of Applied Physics* **73** 1965.
- [8] Wang N, Cao C D, Wei B 1999 *Advances in Space Research*, **24** 1257-1261.
- [9] Zhao S, Li J, Liu L, Zhou Y 2008 *Journal of Alloys and Compounds* **478** 252-256.
- [10] Clopet C R, Cochrane R F, Mullis A M 2012 *Acta Materialia* **61** 6894-6902.
- [11] Herlach D M, Galenko P P K, Holland-Moritz D, Metastable solids from undercooled melts, PERGAMON Press, 2007.
- [12] Wang N, Wei B –B 2004 *Chinese Physics Letters* **21** 1120.
- [13] Schwarz M, Karma A, Eckler K, Herlach D M 1994 *Physical Review Letters* **73** 1380-1383.
- [14] Murray J L 1984 *Metallurgical Transactions a-Physical Metallurgy and Materials Science* **15** 261-268.